Journal of Water Process Engineering 75 (2025) 108026

Contents lists available at ScienceDirect

Journal of Water Process Engineering

journal homepage: www.elsevier.com/locate/jwpe

Ti-$LaFeO_3$ perovskite for enhanced tetracycline degradation and disinfection *via* photo-Fentonreactions: Performance and mechanistic insights

Niloofar Arabbaseri [a], Jorge Rodríguez-Chueca [a], Mahsa Moradi [a], Fernando Fresno [b], Pilar García-Armada [a], Nicolas Keller [c], Patricia García-Muñoz [a,*]

[a] Department of Industrial Chemical & Environmental Engineering, Escuela Técnica Superior de Ingenieros Industriales, Universidad Politécnica de Madrid, C/José Gutiérrez Abascal 2, 28006 Madrid, Spain
[b] Instituto de Catálisis y Petroleoquímica (ICP), CSIC, C/ Marie Curie 2, 28049 Madrid, Spain
[c] Institut de Chimie et Procédés pour l' Energie, l' Environnement et la Santé, ICPEES, CNRS, University of Strasbourg, 25 rue Becquerel, 67087 Strasbourg, France

ARTICLE INFO

Editor: Luca Fortunato

Keywords:
Contaminants of emerging concern (CECs)
Disinfection
Photocatalysis
Advanced oxidation processes (AOPs)
CWPO
Wastewater

ABSTRACT

The presence of contaminants of emerging concern (CECs) along with pathogenic microorganisms poses a significant environmental and health concern. In this study, Ti-$LaFeO_3$ was investigated for the activation of two oxidants: hydrogen peroxide (H_2O_2) and peroxymonosulfate (PMS) in presence of solar light towards simultaneous degradation of tetracycline (TC) and disinfection of wastewater. Heterogeneous catalytic wet peroxide oxidation (CWPO), which relies on the catalytic breakdown of H_2O_2, or more recently PMS, in the presence of metal ions such as typically iron, and photocatalysis, which exploits the redox properties of semiconductors under light irradiation, have both garnered significant attention for their high efficiency and relatively low cost. The effects of solution pH, catalyst and oxidants concentration, were comprehensively investigated. The highest degradation of TC was observed after 120 min in the presence of PMS and solar radiation at alkaline pH and 0.1 g/L Ti-$LaFeO_3$. Furthermore, the impact of common water anions such as chloride, phosphate, carbonate and nitrate, was evaluated on the TC degradation. Last but not least, scavenging tests revealed that hydroxyl and sulfate radicals were the dominant reactive oxygen species (ROS) responsible for the TC degradation in both Solar/Ti-$LaFeO_3$/PMS and Solar/Ti-$LaFeO_3$/H_2O_2 processes. In general, $^{\bullet}OH$ is the most reactive but non-selective species, strongly interacting with tert-butyl alcohol, methanol, and benzoic acid, while $^1O_2$ is the least reactive but highly selective, with NaN_3 as its primary scavenger.

1. Introduction

Environmental pollution has given rise to numerous health issues affecting people globally. Water is an invaluable resource essential for sustaining life. With the global population on the rise, water resources are becoming increasingly scarce, and water pollution has emerged as a significant concern. Wastewater containing various contaminants of emerging concern (CECs) is subject to treatment processes before being released into the environment. The occurrence of refractory pollutants and the scarcity of water continue to be pressing challenges [1]. As a category CECs, pharmaceuticals and personal care products (PPCPs) have been ubiquitously detected in water bodies. In recent years, there has been a lot of attention to PPCPs, since their presence in water resources imposes threats to the environment and human health [2,3]. In everyday life, PPCPs are introduced into water bodies through pipelines or direct release into the environment. Among these, antibiotics like tetracycline (TC)—the second most produced and consumed antibiotic globally—pose a significant concern due to their persistence and potential health risks. The release of TC into natural ecosystems represents a major environmental and public health threat, as it is highly chemically stable and resistant to biological degradation. These characteristics make its removal from water sources particularly challenging, requiring the application of various purification methods and advanced treatment technologies [4,5].

Various treatment processes can be applied for the elimination of such pollutants from wastewater treatment plants (WWTPs) effluents

* Corresponding author.
E-mail address: patricia.gmunoz@upm.es (P. García-Muñoz).

https://doi.org/10.1016/j.jwpe.2025.108026
Received 14 April 2025; Received in revised form 22 May 2025; Accepted 26 May 2025
Available online 2 June 2025

such as adsorption [6], membrane processes [7], biological processes [8], as well as the advanced oxidation processes (AOPs) [9]. AOPs are based on the generation of highly reactive chemical species through the reactions between oxidants, catalysts, and activators such as UV radiation [10], solar radiation, ultrasound [11], etc. Photocatalysis and photo-Fenton processes are among promising advanced photochemical oxidation processes, the combination of which can bring about synergistic effects in degradation of CECs [12]. The Fenton process generally relies on reaction of an oxidant (typically H_2O_2) and a catalyst (most commonly Fe^{2+}) at acidic pH leading to generation of reactive oxygen species (ROS), especially hydroxyl radical ($^{\bullet}OH$) [13]. Fenton process can be enhanced by addition of an activator like solar energy for photolysis of source oxidant e.g. H_2O_2 as well as Fe $(OH)^{2+}$ or $FeOH^{+}$. Besides, photo-reduction of Fe^{3+} to Fe^{2+} improves the regeneration of catalyst through more generation of $^{\bullet}OH$ [13]. Photocatalysis, a form of advanced oxidation process (AOP), relies on light-sensitive materials to trigger chemical reactions that produce powerful oxidizing agents like hydroxyl radicals ($^{\bullet}OH$) and superoxide ions ($^{\bullet}O_2^-$). These reactive species can break down stubborn organic pollutants into harmless substances such as carbon dioxide and water. Materials like metal oxides and ferrites, known as semiconductor photocatalysts, are especially effective because they promote electron movement and redox reactions when exposed to light. Thanks to its efficiency, low energy requirements, and minimal environmental impact, photocatalysis has become a promising approach for treating contaminated wastewater [14,15].

Likewise, application of catalytic wet peroxide oxidation (CWPO) or heterogeneous Fenton process using water-insoluble solid catalysts can overcome the drawbacks of the homogeneous Fenton processes by eliminating significant iron leach into the solution, thereby decreasing the sludge generation, and providing a more durable catalyst [16]. Solar photocatalysis is another category of AOPs which can take the advantage of solar radiation as a durable energy resource to produce reactive oxygen species (ROS). In this way, solar light harvesting at the surface of a catalyst with narrow band gap can lead to transfer of electrons from the valence band to the conduction band generating ROS to degrade the organic contaminants [17]. $LaFeO_3$ is a p-type perovskite semiconductor with a narrow band gap (2.1–2.7 eV), making it a promising catalyst. It is widely known for its magnetic, electrical, and catalytic properties, which make it suitable for applications such as solid oxide fuel cells, gas sensors, and photocatalysts. Its photocatalytic performance can be enhanced by partially replacing La or Fe cations [18]. Catalytic Wet Peroxide Oxidation (CWPO) is an efficient and cost-effective advanced oxidation process for wastewater treatment, utilizing metal-based catalysts, primarily iron, to activate hydrogen peroxide (H_2O_2) and generate ROS for pollutant degradation [12]. It operates under mild conditions, reduces sludge formation, and minimizes catalyst deactivation. Perovskite-type catalysts like $LaFeO_3$ are promising due to their redox properties, thermal stability, and tunable structure. $LaFeO_3$ effectively activates H_2O_2, producing hydroxyl radicals ($^{\bullet}OH$), and modifications such as metal doping enhance its efficiency [13].

Over the past few years, peroxymonosulfate (PMS) has emerged as an effective alternative oxidant in AOPs. PMS activation leads to the generation of sulfate radicals ($SO_4^{\bullet-}$), which are highly reactive and exhibit a longer half-life compared to hydroxyl radicals. These characteristics make PMS-based systems particularly effective in degrading resistant pollutants like tetracycline. Additionally, PMS can be activated under mild conditions using catalysts or light, offering flexibility in process design and improving overall treatment efficiency [19].

In this pioneering study, the Ti-$LaFeO_3$/PMS and Ti-$LaFeO_3$/H_2O_2 systems were investigated for the first time under solar irradiation, aiming at the simultaneous degradation of tetracycline (TC) and inactivation of *Enterococcus faecalis* in simulated urban wastewater. Key operational parameters - including oxidant and catalyst concentrations, as well as solution pH - were systematically optimized. To better reflect real world conditions, the influence of typical water anions was examined, providing valuable insights into matrix effects. Reactive oxygen species (ROS) scavenging experiments were conducted to elucidate the dominant oxidative pathways. Collectively, this work offers a comprehensive evaluation of solar-driven advanced oxidation processes for dual-action water treatment.

2. Materials and methods

2.1. Materials

Throughout the study, different types of chemical reagents are used for various purposes. For the synthesis of the catalyst, $Fe(NO_3)_3$ nonahydrate (Sigma-Aldrich), $La(NO_3)_3$ hexahydrate (Sigma-Aldrich), citric acid ($C_6H_8O_7$,Sigma-Aldrich), titanium tetraisopropoxide (TTIP, Sigma-Aldrich) and Aeroxide TiO_2 P25 (hydrophilic fumed titanium oxide, Evonik,) were used. Additionally, two different oxidants were used in combination with the synthetized catalyst, namely PMS ($2KHSO_5{\cdot}KHSO_4{\cdot}K_2SO_4$, Sigma-Aldrich) and H_2O_2 (30 % *v*/v; Chem-Lab) in a concentration range of 0.55–1.1 mM.

On the other hand, it was required different reagents to prepare the simulated wastewater sample (SWW) according to the OECD Guidelines for the Testing of Chemicals, Simulation Test- Aerobic Sewage Treatment: 303 A (1999). This aqueous matrix was used due to its similarity in physicochemical properties with a real treated wastewater sample, with the advantage of having a constant composition and not requiring sampling from the treatment plants: SWW was prepared by dissolving the following materials in deionized water: Meat peptone (Sharlau) = 32 mg/L, Meat extract (Sharlau) = 22 mg/L, Urea synthesis grade (CH_4N_2O, Sharlau) = 6 mg/L, sodium chloride (NaCl, Sharlau) = 7 mg/L, calcium chloride dehydrate ($CaCl_2{\cdot}2H_2O$, Sharlau) = 4 mg/L, magnesium sulfate heptahydrate ($MgSO_4{\cdot}7H_2O$, Sharlau) = 2 mg/L, and potassium hydrogen phosphate (K_2HPO_4, Sharlau) = 28 mg/L.

To determine the radical species involved in the decontamination and disinfection processes, a set of scavengers is used. The concentration used for scavengers is 5 times the concentration the antibiotic (TC) concentration. *Tert*-butyl alcohol (TBA, $C_4H_{10}O$, Scharlau), methanol (MeOH, CH_3OH, Chem-Lab), Benzoic acid (BA, $C_7H_6O_2$) and Sodium azide (SA, NaN_3) were supplied from Sigma Aldrich. In our experiment, TBA and MeOH are both effective at capturing hydroxyl radicals ($^{\bullet}OH$), helping to identify their role in chemical reactions. Similarly, BA interacts with hydroxyl radicals and is often used to measure their concentration. On the other hand, SA is mainly used to neutralize singlet oxygen ($^1O_2$) but can also react with other reactive oxygen species, like superoxide ($O_2^{\bullet-}$). Finally, different inorganic salts were used to determine the matrix effect of the proposed treatments. In this way, NaCl, Sodium nitrate ($NaNO_3$), K_2HPO_4 and Sodium carbonate anhydrate (Na_2CO_3) were supplied from Sigma Aldrich and the concentration that it used is 5 mM.

2.2. Synthesis of Ti-$LaFeO_3$

The as-made Ti-$LaFeO_3$ was synthesized using a modified sol-gel Pechini method as explained in our previous study [16]. In brief, lanthanum nitrate hexahydrate and iron nitrate nano hydrate were dissolved in 30 mL distilled water at 3.25 g/L and 4.1 g/L, respectively, and the metallic ions underwent complexation by subsequent addition of citric acid ($C_6H_8O_7$, 2.1 g/L) in a stoichiometric molar ratio with respect to the metallic ions [20]. Precise quantities of TiO_2 Aeroxide P25 were gradually added to the aqueous solution while stirring, and the resulting suspensions were kept at 80 °C for 24 h (with a heating rate of 2 °C per minute) to ensure complete gel formation. The dried gel was calcined following the heating procedure outlined by Gosavi et al. [21], with a heating rate of 5 °C per minute. The temperature was held at 600 °C for 2 h, followed by a plateau at 800 °C for 3 h.

Eq. 1 shows the stoichiometric reaction forming the $LaFeO_3$ perovskite:

$$La(NO_3)_3x6H_2O + Fe(NO_3)_3x9H_2O + C_6H_8O_7xH_2O \rightarrow LaFeO_3 + 6CO_2 + 3N_2 + nH_2O \quad (1)$$

2.3. Techniques for structural characterization of Ti-$LaFeO_3$

The electrochemical characterization was carried out with an Eco-chemie BV Autolab PGSTAT 12. The measurements were performed in a photoelectrochemical three-electrode cell with nominal exposure area of 1 cm^2, at room temperature, with a modified FTO as working electrode, a Pt wire as auxiliary electrode and a Ag/AgCl reference electrode. The electrolyte used was a 0.1 M Na_2SO_4 solution. The Electrochemical Impedance Spectroscopy measurements (EIS) parameters used were frequency range 0.01 Hz to 1 MHz, AC amplitude 5 mV. The solutions for cyclic voltammetry were deoxygenated by purging with high-purity nitrogen.

Preparation of modified FTO electrode: 0.7 mg of the suitably ground material were suspended in 1 mL of diluted nafion (1:100 in absolute ethanol) and sonicated for ten minutes to achieve a uniform suspension. Next, 50 mL of the mixture was dropped onto the surface of the FTO and allowed to air dry.

2.4. Analytical and microbiological methods

For the determination of TC in the samples, an Agilent 1260 Infinity II LC System HPLC/VWD was employed, with a ZORBAX Eclipse Plus C18 (4.6 × 100 mm, 5 μm) column as a stationary phase and a 2 % acetic acid in H_2O/acetonitrile 85:15 at 1.5 mL/min as a mobile phase, with no temperature control. The absorption wavelength was fixed at 276 nm. TC concentration determinations were carried out by duplicate.

While, for the experiments focusing on disinfection efficiency, a fresh liquid culture of *Enterococcus faecalis* (ATCC 29212, Scharlab). was prepared in Luria-Bertani nutrient medium (LB broth, Scharlau) and incubated for 20 h at 37 °C. The bacterial suspension was harvested by centrifugation at 4,500 rpm for 15 min. The bacterial pellet was re-suspended in a sterile saline solution (NaCl 0.9 %) providing ca. 10^9 CFU/mL of *E. faecalis* and diluted in the synthetic wastewater to an approximate initial concentration in the range of 10^5–10^6 CFU/mL right before starting the experiment. Thereafter, for the quantification of *E. faecalis*, drop plate and spread plate methods were used. Initially, the collected samples were diluted using serial 10-fold dilution in sterile saline solution and cultured on Slanetz&Bartley (Condalab) agar medium in Petri dishes followed by incubation at 37 °C for 48 h. Afterwards, the colonies were counted and reported in CFU/mL. The detection limit (DL) was in the range of 10 and 100 CFU/mL depending on culture method used [22].

2.5. Experimental procedure

The photocatalytic reactions were conducted in a 250 mL Pyrex reactor on a magnetic stirrer. A solar chamber (ATLAS SUNTEST CPS+) with a 6.876 W/m^2 lamp was used as solar radiation source. In each set of experiments, the reactor was loaded with 100 mL of SWW and containing 10 ppm of TC to study the performance and applicability of the prepared Ti-$LaFeO_3$ for water disinfection, SWW containing TC was inoculated with *E. faecalis* having an initial concentration of ca. 10^6 CFU/mL. At each reaction time, 1 mL sample was taken for microbial analysis. After addition of specific amounts of catalyst and/or oxidant, the reaction was started and samples were withdrawn for analysis in different time intervals. To evaluate the process efficiency, TC degradation was investigated under varying levels of independent variables including the solution pH, concentration of the as-made Ti-$LaFeO_3$, as well as oxidant type (PMS or H_2O_2) and concentration. In selected conditions of each oxidant, process efficiency was evaluated in presence of common anions of water including sulfate, chloride, carbonate and nitrate. Besides, MeOH, TBA, SA and BA were used as scavengers to investigate the degradation mechanisms and domination of ROS in photocatalytic reactions. To evaluate the durability of the as-made catalyst, reuse experiments were conducted by filtering the reactor content at the end of the experiment followed by catalyst separation, washing with deionized water and drying in oven at less than 100 °C.

3. Results and discussions

3.1. Catalyst characterization

The main physico-chemical properties of the Ti-$LaFeO_3$ catalyst can be found in García-Muñoz et al. [16]. Fig. S1 shows the XRD pattern with Rietveld structural refinement. Briefly, the photocatalyst exhibits a crystalline structure with an average particle size of 21 nm and a surface area of 5 m^2/g. Rietvelt refinements indicate a Ti substitution rate of 11 % within the $LaFeO_3$ lattice. In Fig. S2, the Tauc plot derived from the UV–vis diffuse reflectance spectra allows for the estimation of the band gap at 2.1 eV. Fig. S3 shows the fluorescence decay curve, indicating a photogenerated charge carrier lifetime of 2.70 ns. Fig. S4 shows a representative SEM image of the material.

For a more detailed characterization, (photo-)electrochemical runs were performed. The cyclic voltammogram (Fig. 1) shows a quasi-reversible system with anodic and cathodic potentials of 0.375 V and 0.181 V respectively, and formal potential $E^{0'} = 0.278$ V. The number of electrons exchanged by this electrochemical system, calculated from the peak width at mid-heigh [23], was $n = 1$. The average surface electroactive coverage, estimated from the integrated charge of the voltammetric waves was $8.08 \cdot 10^{-15}$ mol cm^{-2}.

Fig. 2 shows a near-rectangular and symmetric shape suggesting a fast electron transfer indicative of reversible redox system and desirable in applications as is the case for (photo-)catalytic applications [24,25].

The EIS (Nyquist) plot shows a semi-circle indicative of a charge transfer resistance (R_{CT}) at the interface electrode-electrolyte (Fig. 3). The Bode plot let us estimate the lifetime (τ) of electrons generated in the anode [26], by the equation:

$$\tau = \frac{1}{2\pi f_{max}}$$

Being f_{max} the maximum frecuency. The calculated lifetime was 399.79 ms, notably higher than other reported materials based on iron oxides doped with lanthanum [27].

The Mott-Schottky plot (Fig. 4) shows a positive slope ($1.684 \cdot 10^9$) indicating that the semiconductor material is n-type [28]. This plot allows us to calculate the flat-band, E_{FB} potential from the intercept on the

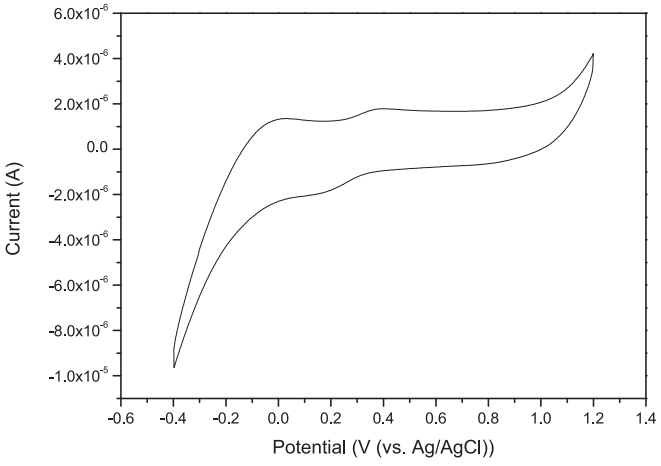

Fig. 1. Cyclic voltammogram of FTO electrode modified with the material. Scan rate 20 mV s^{-1}.

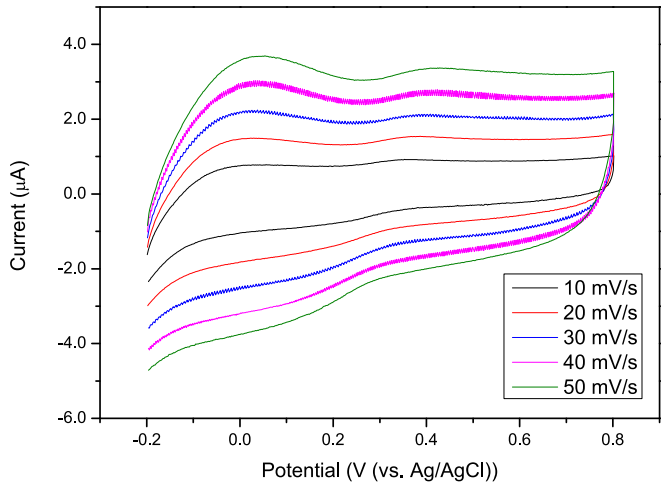

Fig. 2. Dependence of the peak current on the scan rate of modified FTO electrode.

x-axis [4]. The obtained value was - 0.63 V, indicative of a high-energy Fermi level [29], confirmed by the considerable shift in OCP (Open Circuit Potential) caused by illumination of the electrode with 371 nm light (Fig. 5).

3.2. *Photocatalytic degradation of TC in solar/TiLaFeO$_3$/oxidant systems*

3.2.1. *Effect of oxidant type and concentration*

In this step, the solar/Ti-LaFeO$_3$/oxidant system was evaluated using either H_2O_2 or PMS as the oxidant at concentrations of 0.55 mM, 1.1 mM, and 2.2 mM, with a Ti-LaFeO$_3$ catalyst concentration of 0.250 g/L, and the results are graphically depicted in Fig. 6.

As shown in Fig. 6(a), the highest TC degradation occurred with 1.1 mM H_2O_2 after 120 min of reaction. In contrast, when PMS was used instead of H_2O_2, the optimal concentration for TC degradation was 0.55 mM, as seen in Fig. 6(b).

In the presence of H_2O_2, the 1.1 mM concentration proved to be the most effective for TC degradation compared to other tested concentrations. Generally, increasing oxidant concentrations enhances reactive oxygen species (ROS) generation, leading to higher degradation rates. However, an optimal balance must be maintained to maximize efficiency. At 1.1 mM, H_2O_2 interacts effectively with both the Ti-LaFeO$_3$ catalyst and solar irradiation, generating a sufficient amount of hydroxyl radicals ($^{\bullet}OH$) to drive pollutant removal. In contrast, a lower concentration (0.55 mM) may not produce enough radicals, resulting in a slower degradation process. On the other hand, an excessive concentration (2.2 mM) can lead to radical scavenging, where surplus H_2O_2 reacts with hydroxyl radicals instead of enhancing the degradation process, ultimately reducing efficiency [20]. The optimal H_2O_2 concentration identified in this study aligns with the findings of García-Muñoz et al. [30], who reported a comparable optimal dosage when using a

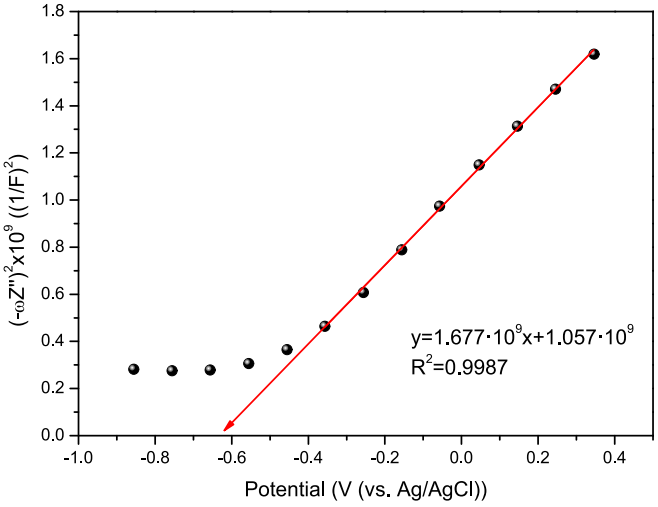

Fig. 4. Mott-Schottky plot for the FTO modified electrode.

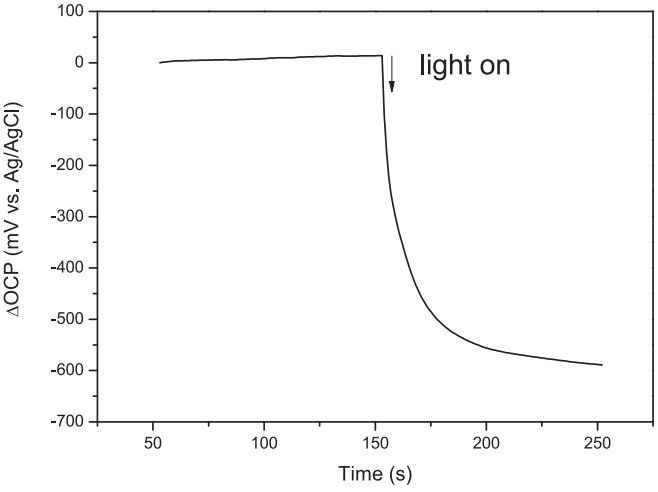

Fig. 5. $\Delta OCP = OCP_{illuminated} - OCP_{dark}$

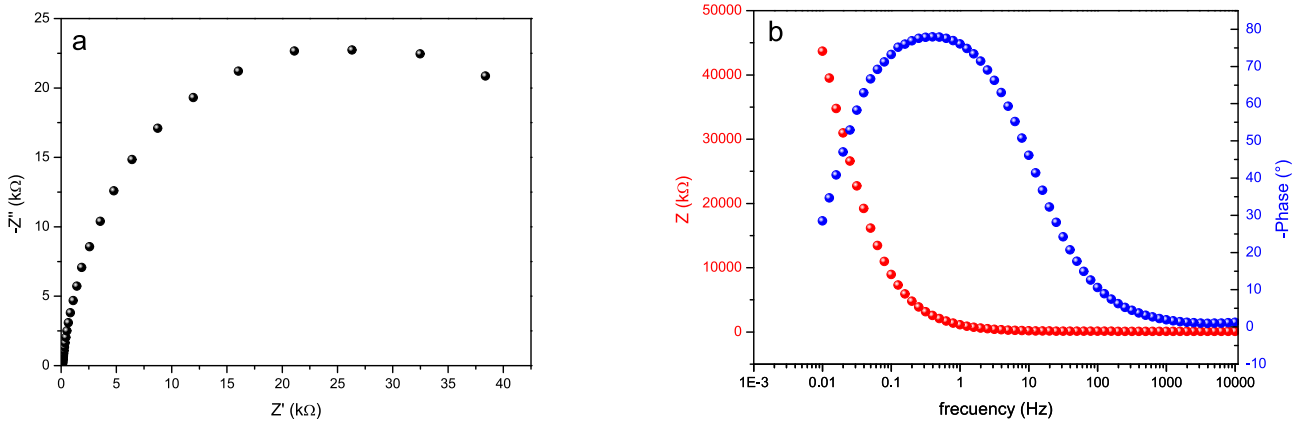

Fig. 3. (a) Nyquist plot of the FTO modified electrode, and (b) the corresponding Bode plot.

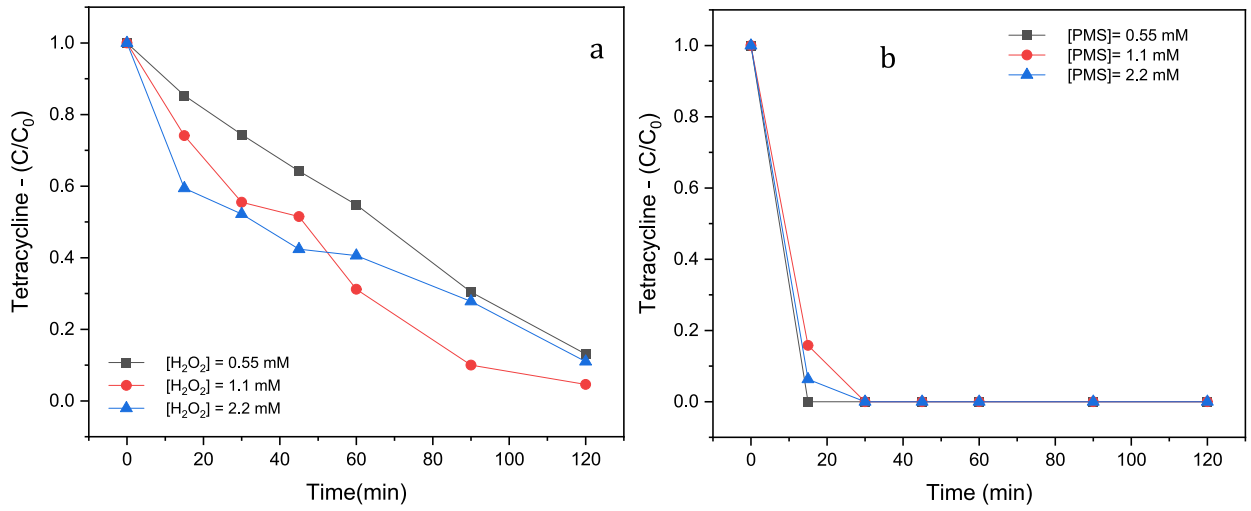

Fig. 6. Effect of oxidant concentration on TC degradation in (a) solar/Ti-LaFeO$_3$/H_2O_2 and (b) solar/Ti-LaFeO$_3$/PMS systems (pH = 3, [Ti-LaFeO$_3$] = 0.250 g/L, [TC] = 10 mg/L). Both in SWW matrix.

similar catalyst and oxidant. This consistency suggests that the selected concentration effectively maximizes reactive species generation while maintaining catalytic efficiency. Fig. 6(b) illustrates that higher PMS concentrations (1.1 mM and 2.2 mM) generate excessive reactive oxygen species (ROS), leading to oxidative stress beyond the optimal level for TC degradation [31,32]. This finding contrasts with the results of Wang et al., who observed an increase in TC degradation efficiency with higher PMS dosages in their experiments [31]. The optimal PMS concentration of 0.55 mM strikes a balance between efficient radical production and minimizing scavenging effects. PMS (peroxymonosulfate, HSO_5^-) is activated by Ti-LaFeO$_3$ and solar irradiation, producing sulfate radicals ($SO_4^{\bullet-}$) and hydroxyl radicals ($^{\bullet}OH$), which are crucial for pollutant degradation. At 0.55 mM, there is a sufficient amount of PMS to generate reactive species without excessive accumulation, ensuring effective TC removal. Moreover, excessive PMS can interfere with the catalyst's surface activity, leading to competitive adsorption and diminishing the efficiency of oxidant activation. Thus, the 0.55 mM PMS concentration provides the best balance, maximizing radical generation while maintaining catalyst effectiveness and preventing unnecessary oxidant consumption.

3.2.2. *Effect of catalyst concentration*

The effect of different Ti-LaFeO$_3$ catalyst concentrations, combined with previously selected amounts of either PMS or H_2O_2, on TC removal was studied, and the results shown in Figs. 7(a) and 7(b) respectively.

In the solar/Ti-LaFeO$_3$/H_2O_2 system, an increase in catalyst concentration led to a decrease in TC removal efficiency with an optimal amount of catalyst is 0.1 g/L. This effect, influenced solely by the catalyst and solar irradiation, can be attributed to increased solution turbidity, which reduced light penetration at higher catalyst concentrations [33]. This phenomenon is similar to the findings of Soltanabadi et al., where an increased catalyst concentration can lead to the deactivation of activated molecules due to agglomeration. This, in turn, reduces the penetration of radiated light, increases radiation scattering, and ultimately lowers the decolorization efficiency [13].

When the catalyst concentration exceeds an optimal threshold, the denser particle suspension blocks light, a phenomenon known as “light shielding”. Since light is crucial for activating the photocatalytic process, this obstruction limits photon absorption and ultimately reduces reaction efficiency. Similar results have been reported by Karaca et al. [34]. Salari et al. reported that an excessive amount of photocatalyst adversely impacts photoactivity. At high photocatalyst concentrations, photoactivity declines due to light scattering and particle ablation [35].

3.2.3. *Performance comparison with control experiments*

Fig. 8 graphically represents and compares the TC removal results from the optimized solar/catalyst/oxidant treatments discussed in the previous sections with the control experiments.

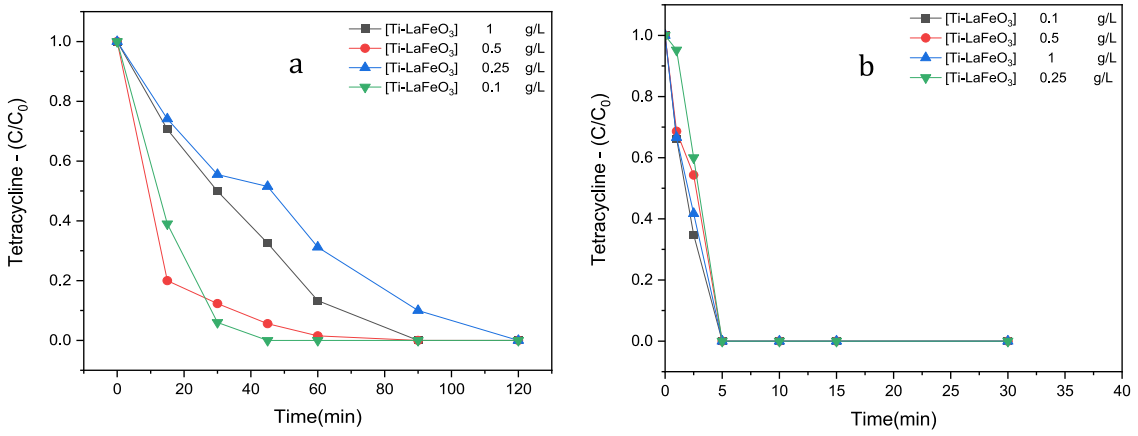

Fig. 7. Effect of Ti-LaFeO$_3$ concentration on TC degradation in (a) solar/TiLaFeO$_3$/H_2O_2 and (b) solar/Ti-LaFeO$_3$/PMS systems (pH = 3, [TC] = 10 mg/L, [H_2O_2] = 1.1 mM, [PMS] = 0.55 mM). Both in SWW matrix.

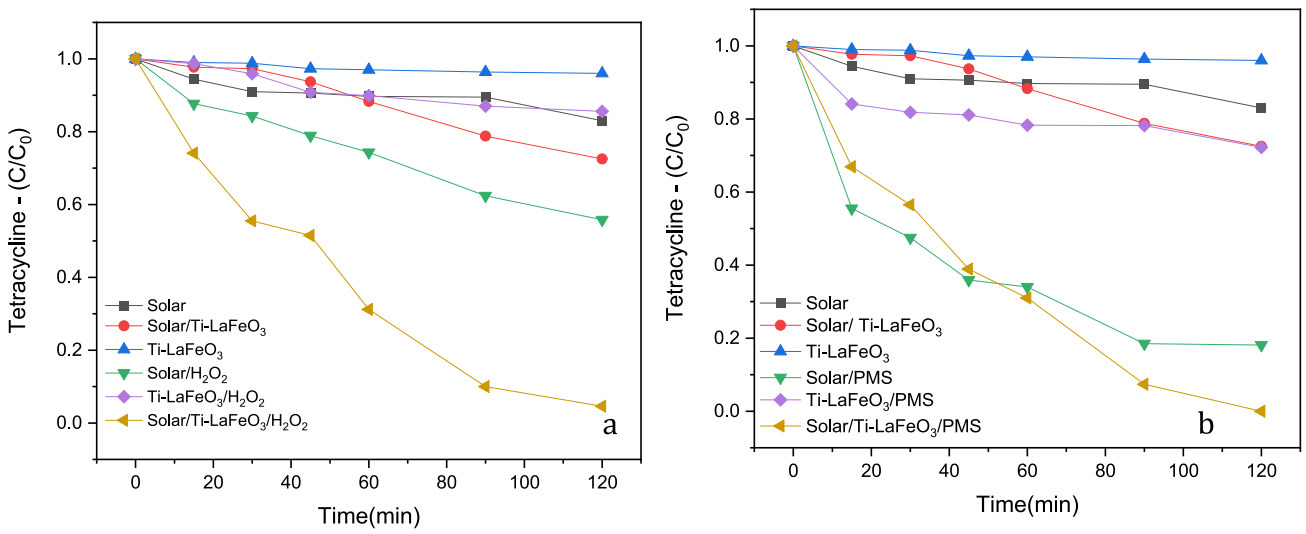

Fig. 8. Control experiments on TC degradation, (a) solar/TiLaFeO$_3$/H_2O_2 and (b) solar/Ti-LaFeO$_3$/PMS systems (pH = 3, [TC] = 10 mg/L, [H_2O_2] = 1.1 mM, [PMS] = 0.55 mM). Both in SWW matrix.

In the control tests, the synergistic effect was evaluated not only by analyzing each factor individually but also in combination with one of the most effective parameters. As shown in Fig. 8, individual agents such as solar radiation, the catalyst, or oxidants alone had limited efficiency in TC removal. However, when solar radiation, the catalyst, and an oxidant (especially PMS) were combined, the removal efficiency increased significantly, highlighting a strong synergistic effect between the three components.

$$S_{123} = \frac{K_{123}}{K_1 + K_2 + K_3 + (K_{12} - K_1 - K_2) + (K_{23} - K_2 - K_3) + (K_{13} - K_1 - K_3)} \quad (2)$$

To quantify this synergy, the synergy coefficient was calculated using first-order rate constants, as described in Eq. 2. Each number represents a different variable within the process. For example, k_1 refers to the kinetic constant when only the oxidant is active, while $k_{2/3}$ represents the kinetic constant when both the catalyst and solar radiation are combined. Finally, $k_{1/2/3}$ corresponds to the kinetic constant for the full process, where the oxidant, catalyst, and solar radiation all work together. The results can be observed that processes using PMS and H_2O_2 as oxidants have an S value greater than 1, specifically 1.8 and 1.19, respectively, indicating synergy among the three factors applied in the process in both cases, the synergistic index (S) was greater than 1, meaning the combined effect was approximately three times greater than that of H_2O_2 alone in the presence of PMS, the results shown in Table 1 demonstrate that the system using PMS as the oxidant was the most efficient in terms of energy consumption reinforcing the powerful interaction between these factors similar to the results obtained by Haro et al. [36].

The mineralization rate of tetracycline (TC) was assessed by monitoring the TOC concentration in simulated wastewater. After 120 min, the systems with solar/Ti-LaFeO$_3$/PMS and solar/Ti-LaFeO$_3$/H_2O_2 achieved mineralization rates of 36.2 % and 27.6 %, respectively. This relatively low efficiency suggests that TC primarily breaks down into smaller organic intermediates rather than fully converting to CO_2 and H_2O. Additionally, since the reaction was stopped at 120 min, some persistent organic compounds may still be present, requiring a longer treatment duration for complete mineralization [37,38].

3.2.4. *Effect of solution pH*

Solution pH plays a significant role in TC degradation regarding by influencing the surface charge of the catalyst, the speciation of the matrix ions, and the speciation of ROS. Therefore, effect of different solution pH (3–11) were tested over the optimized conditions for the solar/catalyst/oxidant systems, and the results are graphed in Fig. 9.

As shown in Fig. 9(a)(b), the highest TC removal was achieved at pH = 11 in the solar/Ti-LaFeO$_3$/H_2O_2 process and pH = 9,7 in the system which is solar/Ti-LaFeO$_3$/PMS.

In this study the results obtained are contrary to what reported by Karaca et al. [34] and Wang et al. [31], that Fe-based catalyst (LaFeO$_3$) benefits from acidic conditions, promoting better electron transfer and the production of ROS or in acidic environments, $SO_4^{\bullet-}$ radicals are more likely to interact with deprotonated TC molecules due to their higher electron densities, further accelerating the degradation process. Wang also stated that once $SO^{\bullet}_4$ is generated, it can follow three different pathways: (i) it remains the dominant species at pH levels below 7, (ii) it decomposes into $^{\bullet}OH$ and $SO_4^{\bullet}$ at pH 9, and (iii) it transforms into $^{\bullet}OH$ and SO_4^{2-} at approximately pH 12. This confirms that the highest

Table 1
First-order kinetic constants for systems with one, two, or three variables (oxidant, Ti-LaFeO$_3$, and/or sunlight), synergistic index for the combined system.

Factor	Oxidant (mM)	Ti-LaFeO$_3$ (mg/L)	Sunlight	Oxidant	First-order rate constant (min^{-1})	Synergistic index (S)
1	0.55			PMS	$9.3.10^{-3}$	
1	1.1			H_2O_2	$3.2.10^{-3}$	
1		100			9.10^{-4}	
1			ON		$1.5.10^{-3}$	
2		100	ON		$2.6.10^{-3}$	
2	0.55	100		PMS	$2.16.10^{-2}$	
2	1.1	100		H_2O_2	$1.97.10^{-2}$	
2	0.55		ON		$1.42.10^{-2}$	
2	1.1		ON		$4.8.10^{-3}$	
3	0.55	100	ON	PMS	$2.88.10^{-2}$	1.8
3	1.1	100	ON	H_2O_2	$2.56.10^{-2}$	1.19

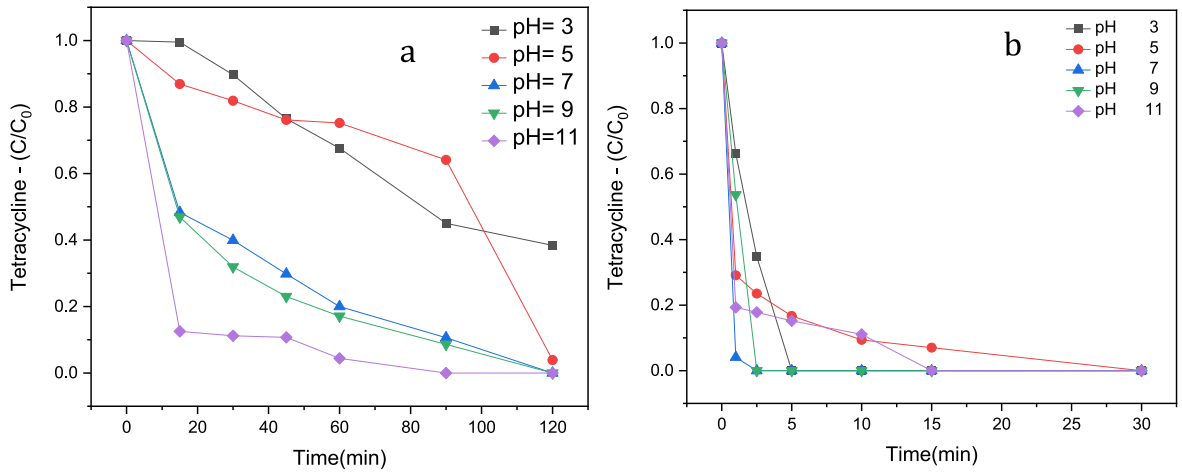

Fig. 9. Effect of pH on TC degradation in solar/Ti-LaFeO$_3$/oxidant systems: (a) solar/Ti-LaFeO$_3$/H$_2$O$_2$ and (b) solar/Ti-LaFeO$_3$/PMS. [TC] = 10 mg/L, [Ti-LaFeO$_3$] = 0.1 g/L, [H$_2$O$_2$] = 1.1 mM, [PMS] = 0.55 mM. Both in SWW matrix.

removal efficiency of organic pollutants is achieved when operating within a pH range of 8 to 12, as this range promotes the presence of more oxidizing radicals. Additionally, it is important to highlight the decomposition of PMS through its alkaline activation, where superoxide radicals and singlet oxygen are identified as the predominant species. Under experimental conditions, since simulated wastewater typically contains buffering agents, mineral ions, and organic pollutants that influence pH, this phenomenon is evident in the studies mentioned above. In particular, industrial and pharmaceutical wastewater simulations often exhibit elevated pH levels due to the presence of ammonia (NH_3/NH_4^+) or phosphate-based buffers, which help maintain alkaline conditions. Consequently, this effect is observed in experiments utilizing both PMS and H_2O_2 as oxidants similar to Tan et al. [39].

3.2.5. *Effect of water matrix*

To evaluate the system's performance in more complex water matrices, reactions were conducted involving various ionic species. This approach helped identify the treatment's limitations when inorganic substances commonly present in different water matrices are involved. The results are represented in Fig. 10.

As shown in Fig. 10 and based on Eqs. 3 and 4, carbonates act as hydroxyl radical ($^{\bullet}OH$) scavengers, reducing the efficiency of pollutant removal. Nitrate ions can absorb UV light and generate nitrogen-containing radicals ($NO_2^{\bullet}$ and $NO_3^{\bullet}$), which contribute to pollutant breakdown [40].

These ions can promote the photolysis of H_2O_2, increasing hydroxyl radical production. As shown in Eqs. 5 and 6 [41]. Phosphate ions can form stable complexes with metal ions, such as Fe^{3+} in the photo Fenton system or La in lanthanum ferrite, restricting their availability for the reaction. These complexes slow down catalysis and reduce the formation of free radicals (Eqs. 7 and 8) [10].

According to Eqs. 9 and 10, the chlorine radicals ($Cl^{\bullet}$ and $Cl_2^{\bullet-}$) produced exhibit oxidizing activity and can effectively remove pollutants, although their oxidation power is lower than that of sulfate or hydroxyl radicals. Kiejza et al. [42]. reported that these three anions act as radical scavengers.

In other words, anions can significantly reduce the efficiency of TC removal in both the H_2O_2 and PMS systems by interfering with ROS production and disrupting catalyst activity.

The Eqs. 3–10 summarize the reactions in solution:

$$SO_4^{\bullet-} + CO_3^{2-} \rightarrow CO_3^{\bullet-} + SO_4^{2-} \quad (3)$$

$$OH^{\bullet} + CO_3^{2-} \rightarrow CO_3^{\bullet-} + OH^- \quad (4)$$

$$NO_3^- + H_2O \xrightarrow{h\nu} NO_2^{\bullet} + OH^{\bullet} + OH^- \quad (5)$$

$$SO_4^{\bullet-} + NO_3^- \rightarrow NO_3^{\bullet} + SO_4^{2-} \quad (6)$$

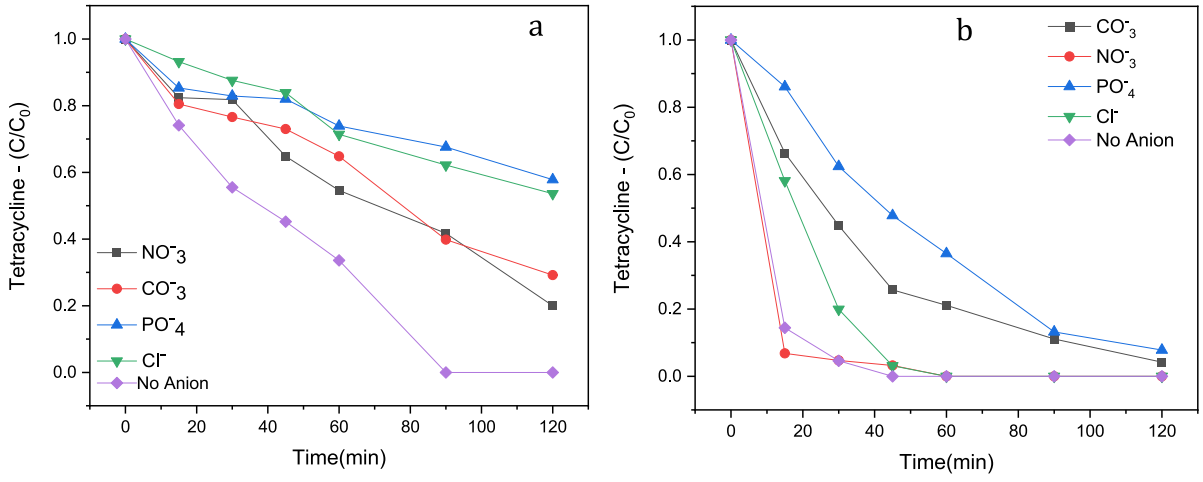

Fig. 10. Effect of the water matrix on TC degradation in Solar/Ti-LaFeO$_3$/oxidant systems: (a) solar/Ti-LaFeO$_3$/H$_2$O$_2$ and (b) solar/Ti-LaFeO$_3$/PMS. Experimental conditions: [Ti-LaFeO$_3$] = 0.1 g/L, [TC] = 10 mg/L, [H$_2$O$_2$] = 1.1 mM, [PMS] = 0.55, pH = 3 mM, [Anions] = 5 mM. Both in SWW matrix.

$$HPO_4^{2-} + OH^{\bullet} \rightarrow HPO_4^{-} + OH^{-} \quad (7)$$

$$HPO_4^{2-} + SO_4^{\bullet -} \rightarrow HPO_4^{-} + SO_4^{2-} \quad (8)$$

$$OH^{-} + Cl^{-} \rightarrow Cl^{\bullet} + OH^{\bullet} \quad (9)$$

$$Cl^{\bullet} + SO_4^{2-} \rightarrow Cl^{-} + SO_4^{\bullet -} \quad (10)$$

3.2.6. Scavenging tests

Several tests were conducted with scavengers to investigate the reaction pathways of the PMS or H_2O_2/Ti-LaFeO$_3$/Solar radiation system and to propose a potential mechanism for the oxidation of TC (Fig. 11). This involved using a group of scavengers that could specifically capture potential free radicals and oxidative species created in the PMS or H_2O_2/Ti-LaFeO$_3$/Solar radiation system, individually.

When MeOH or TBA are added to the reaction system, they scavenge radicals, preventing them from degrading pollutants. MeOH reacts with both hydroxyl ($^{\bullet}$OH) and sulfate ($SO_4^{\bullet -}$) radicals ($k_{\cdot OH/MeOH} = 9.7 \times M^{-1}\cdot s^{-1}$, $k_{SO4-/MeOH} = 2.5 \times 10^7\ M^{-1}\cdot s^{-1}$), inhibiting degradation if these radicals are dominant. TBA selectively targets $^{\bullet}$OH ($k_{\cdot OH/TBA} = 3.8 \times 10^8\ M^{-1}\cdot s^{-1}$); partial inhibition suggests $^{\bullet}$OH plays a key role, while minimal impact implies $SO_4^{\bullet -}$ is more involved [43]. Sodium azide (SA, NaN_3) quenches singlet oxygen ($^1O_2$) and some ROS, with moderate inhibition indicating O_2 participation. Benzoic acid (BA) selectively reacts with $^{\bullet}$OH ($k_{\cdot OH/BA} = 2.35 \times 10^9\ M^{-1}\cdot s^{-1}$); significant inhibition confirms $^{\bullet}$OH as the dominant reactive species [44,45]. The higher kinetic rates of MeOH and TBA cause them to be higher than BA and SA in the graphs. Similar results were obtained by Guerra-Rodríguez and colleagues in the study of the effect of the water matrix on *Enterococcus sp.* inactivation by UV-A activated PMS or H_2O_2 [10].

3.2.7. Reusability of the as-made Ti-LaFeO$_3$

For practical applications, catalysts must demonstrate strong stability. To assess the stability of Ti-LaFeO$_3$, the catalyst particles were recovered and reused three times when using H_2O_2 as the oxidant and five times with PMS. Also, iron leaching was measured at the end of the reactions to corroborate the goodness of the material in the presence of H_2O_2 and PMS. In both cases, no iron leaching was detected, confirming the stability of the catalyst. It is important to note that the detection limit of the ortho-phenanthroline method used is 0.1 mg/L.

Ti-LaFeO$_3$ showed good stability, with its removal efficiency decreasing only slightly from 100 % to 90 % over five consecutive cycles with PMS and from 100 % to 44.6 % over three cycles with H_2O_2, as illustrated in Fig. 12.

The reusability assessment of the Ti-LaFeO$_3$ catalyst in solar-assisted oxidation systems using H_2O_2 and PMS as oxidants demonstrated its stability and efficiency for multiple cycles with catalyst recovery by powder filtration. The catalyst retained high removal efficiency, with only a slight decrease from 100 % to 90 % over five consecutive cycles when PMS was used as the oxidant. In contrast, the efficiency declined more significantly, from 100 % to 44.6 %, over three cycles when H_2O_2 was applied. Similar to the reports of García-Muñoz et al. [30] with oxidant and catalyst, except that the experimental conditions were ultrapure water instead of a simulated urban wastewater (SWW). These results highlight the superior performance of PMS in sustaining catalyst activity, likely due to its dual activation by light and catalytic surface interactions. The findings align with previous studies on disinfection, where PMS activation, particularly in the presence of transition metals such as iron, has been shown to generate highly reactive sulfate radicals that enhance degradation efficiency. Additionally, the Ti-LaFeO$_3$ perovskite catalyst has been recognized for its high stability under oxidative conditions, maintaining structural integrity over multiple reaction cycles. This reinforces its potential as a cost-effective and durable catalyst for practical wastewater treatment applications [15]. Overall, the study underscores the importance of selecting an appropriate oxidant to maximize catalyst longevity and treatment efficiency. PMS emerges as the preferred choice for long-term applications due to its sustained activation and radical generation capacity.

3.3. Disinfection study

3.3.1. The effect of simultaneous removal TC/bacteria under optimal operation condition

As shown in Fig. 13, the simultaneous degradation of two pathogens—Tetracycline (TC) and *Enterococcus faecalis*—was investigated using two different oxidants at their optimal concentrations, along with the optimal concentration of the catalyst, each applied separately.

When using both oxidants, the presence of bacteria in the wastewater reduce the activity of the process in terms of TC removal if we compare with the experiments in which the single oxidation of TC was carried out (Fig. 13).

The results demonstrate the enhanced degradation efficiency of tetracycline (TC) and *Enterococcus faecalis* under the optimized solar/Ti-LaFeO$_3$/oxidant system. As shown in Fig. 13, the pollutant removal rate

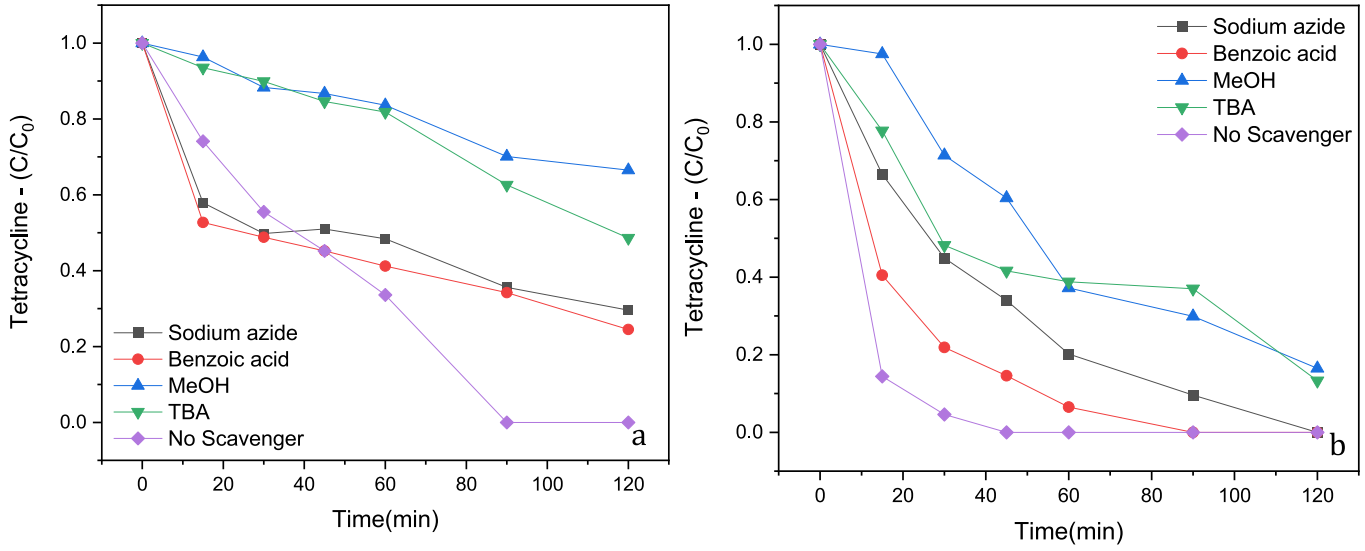

Fig. 11. Effect of different scavengers on TC degradation in Solar/Ti-LaFeO$_3$/oxidant systems: (a) solar/Ti-LaFeO$_3$/H_2O_2 and (b) solar/Ti-LaFeO$_3$/PMS. ([Ti-LaFeO$_3$] = 0.1 g/L, [TC] = 10 mg/L, [H_2O_2] = 1.1 mM, [PMS] = 0.55 mM, [Scavengers] = 0.11 mM. Both in SWW matrix.

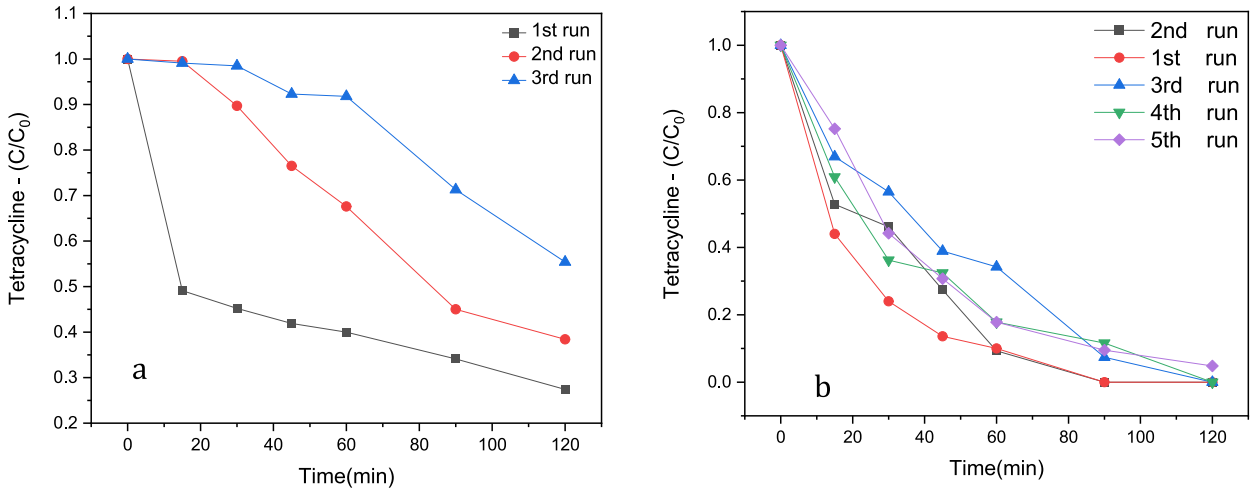

Fig. 12. Reusability test of catalyst in solar/Ti-LaFeO$_3$/oxidant systems: a) H_2O_2 and b) PMS. [Ti-LaFeO$_3$] = 0.1 g/L, pH = 3, [TC] = 10 mg/L, [H_2O_2] = 1.1 mM, [PMS] = 0.55 mM. Both in SWW matrix.

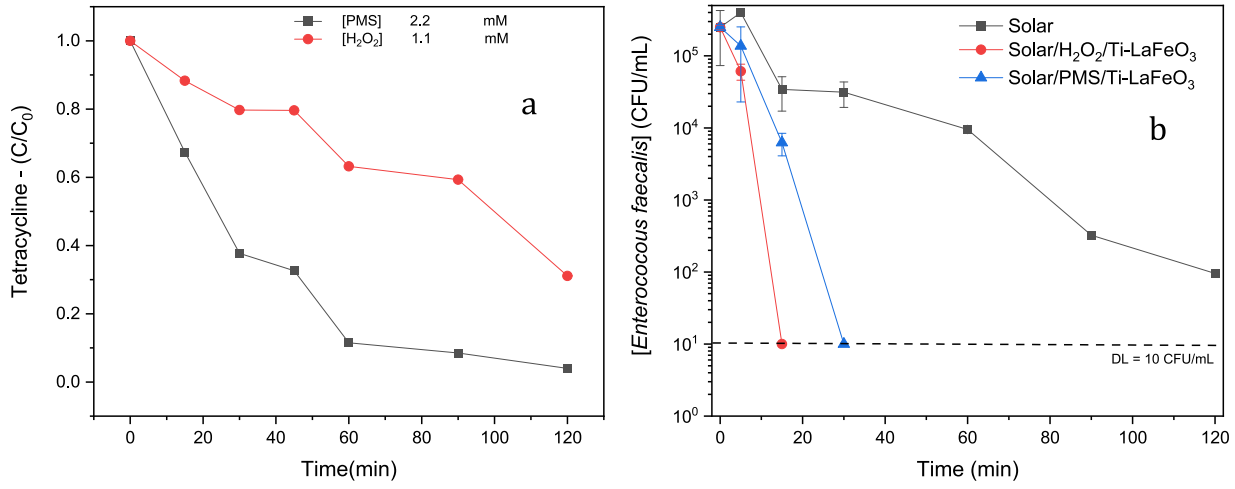

Fig. 13. Effect of degradation TC (a) and Bacteria (b) under optimized treatment solar/Ti-LaFeO$_3$/oxidant. [Ti-LaFeO$_3$] = 0.1 g/L, [H_2O_2] = 1.1 mM, [PMS] = 0.55 mM, [TC] = 10 mg/L. Both in SWW matrix.

increased over time when PMS was used as the primary oxidant, outperforming H_2O_2 in the same catalytic conditions. This phenomenon can be attributed to the dual activation mechanism of PMS, which is influenced not only by the effect of solar irradiation but also by the catalytic activity of the Ti-LaFeO$_3$ surface. The presence of iron within the catalyst has been previously reported to facilitate the activation of sulfate species, leading to the generation of reactive radicals that play a crucial role in the oxidation and disinfection processes [46,47]. All experimental tests followed a consistent degradation trend: an initial phase with a slower pollutant removal rate, followed by a more active phase in which primary degradation occurred. This behavior may be linked to the gradual activation of Fe (III) species on the catalyst surface, which, upon exposure to solar irradiation, undergoes reduction to Fe (II), enhancing the formation of reactive radicals and thereby accelerating the degradation kinetics similar to the work reported by García-Muñoz et al. [15]. Although the highest pollutant removal efficiency was observed with the combination of 0.1 g/L Ti-LaFeO$_3$, 0.55 mM PMS, and solar irradiation, further optimization may allow for reducing catalyst loading while maintaining similar degradation performance. These findings highlight the effectiveness of the solar/Ti-LaFeO$_3$/PMS system as a promising approach for pollutant removal, offering both high efficiency and potential environmental benefits in wastewater treatment applications. Additionally, solar radiation promotes a series of other mechanisms, such as the generation of radicals by breaking the peroxo bond in PMS, the photoreduction of the metal, or those associated with the catalyst itself with photocatalytic capacity [20]. Previous studies have totally removed bacteria population in similar reaction time but with much lower concentrations [48].

4. Conclusions

A new combined process using PMS, solar radiation and Ti-LaFeO$_3$ catalyst has been employed for simultaneous TC/bacteria removal in simulated urban wastewater treatment. This treatment has demonstrated high activity for TC removal (100 % in 120 min), complete disinfection as well as high stability showed through 5 cycles of reaction with a slight loss of activity. Besides, the combined process showed a synergistic effect value of 1.08. The mechanistic study performed with several scavengers demonstrated that the main active radical species were $^{\bullet}OH$ and $SO_4^{\bullet-}$.

CRediT authorship contribution statement

Niloofar Arabbaseri: Methodology, Investigation, Formal analysis. **Jorge Rodríguez-Chueca:** Writing – original draft, Validation, Supervision, Methodology, Investigation, Funding acquisition, Data curation,

Conceptualization. **Mahsa Moradi:** Investigation, Formal analysis, Data curation. **Fernando Fresno:** Investigation, Validation. **Pilar García-Armada:** Investigation. **Nicolas Keller:** Validation, Formal analysis. **Patricia García-Muñoz:** Writing – original draft, Validation, Supervision, Methodology, Investigation, Funding acquisition, Data curation, Conceptualization.

Declaration of competing interest

The authors declare that they have no known competing financial interests or personal relationships that could have appeared to influence the work reported in this paper.

Acknowledgements

This work has received financial support from Spanish MCIN/AEI/10.13039/501100011033 and "ERDF A way of making Europe", through project PHOTORAS (PID2021-128165OA-I00. PGM acknowledges Comunidad de Madrid through the call Research Grants for Young Investigators from Universidad Politécnica de Madrid for funding the research project SUNCAT4PLAST (APOYO-JOVENES-21-JV4DEB-3-Q2WGKV).

Appendix A. Supplementary data

Supplementary data to this article can be found online at https://doi.org/10.1016/j.jwpe.2025.108026.

Data availability

Data will be made available on request.

References

[1] Q. Cheng, G.-K. Zhang, Enhanced photocatalytic performance of tungsten-based photocatalysts for degradation of volatile organic compounds: a review, Tungsten 2 (2020) 240–250.
[2] N. Wang, G. Kang, G. Hu, J. Chen, D. Qi, F. Bi, N. Chang, Z. Gao, S. Zhang, W. Shen, Spatiotemporal distribution and ecological risk assessment of pharmaceuticals and personal care products (PPCPs) from Luoma Lake, an important node of the south-to-north water diversion project, Environ. Monit. Assess. 195 (2023) 1330.
[3] T. Yan, Q. Ping, A. Zhang, L. Wang, Y. Dou, Y. Li, Enhanced removal of oxytetracycline by UV-driven advanced oxidation with peracetic acid: insight into the degradation intermediates and N-nitrosodimethylamine formation potential, Chemosphere 274 (2021) 129726.
[4] I. Berruti, S. Nahim-Granados, M.J. Abeledo-Lameiro, I. Oller, M.I. Polo-López, Recent advances in solar photochemical processes for water and wastewater disinfection, Chemical Engineering Journal Advances 10 (2022) 100248.
[5] J. Yang, Y. Lin, X. Yang, T.B. Ng, X. Ye, J. Lin, Degradation of tetracycline by immobilized laccase and the proposed transformation pathway, J. Hazard. Mater. 322 (2017) 525–531.
[6] H. Yu, M. Tang, J. He, C. Liu, P. Wu, W. Jiang, Intelligent treatment of tannery wastewater via H2O2 photocatalytic oxidation coupled adsorption process, Journal of Water Process Engineering 63 (2024) 105378.
[7] T. Poerio, C. Lavorato, A. Severino, B. Russo, R. Molinari, P. Argurio, A. Figoli, Combined membrane separation and photocatalysis process for the recovery and decomposition of micro/nanoplastics from polyester fabrics, J. Environ. Chem. Eng. 12 (2024) 113310.
[8] C. Morim, J.P. Ribeiro, F.C. Silva, M.I. Nunes, Two-stage treatment of pulp bleaching wastewater by Fenton and biological processes to remove recalcitrant pollutants, Journal of Water Process Engineering 63 (2024) 105451.
[9] M.A. Iqbal, S. Akram, B. Lal, S.U. Hassan, R. Ashraf, G. Kezembayeva, M. Mushtaq, N. Chinibayeva, A. Hosseini-Bandegharaei, Advanced photocatalysis as a viable and sustainable wastewater treatment process: a comprehensive review, Environ. Res. 253 (2024) 118947.
[10] S. Guerra-Rodríguez, E. Rodríguez, J. Moreno-Andres, J. Rodriguez-Chueca, Effect of the water matrix and reactor configuration on *Enterococcus* sp. inactivation by UV-A activated PMS or H_2O_2, J. Water Process Eng. 47 (2022) 102740.
[11] S. Malato, P. Fernández-Ibáñez, M.I. Maldonado, J. Blanco, W. Gernjak, Decontamination and disinfection of water by solar photocatalysis: recent overview and trends, Catal. Today 147 (2009) 1–59.
[12] L. Liu, Z. Shen, C. Wang, Recent advances and new insights on the construction of photocatalytic systems for environmental disinfection, J. Environ. Manag. 353 (2024) 120235.
[13] Y. Soltanabadi, M. Jourshabani, Z. Shariatinia, Synthesis of novel CuO/LaFeO3 nanocomposite photocatalysts with superior Fenton-like and visible light photocatalytic activities for degradation of aqueous organic contaminants, Sep. Purif. Technol. 202 (2018) 227–241.
[14] R. Zhao, X. Yang, T. Li, T. Yu, F. Chen, Z. Shen, The application of diatomic catalysts in advanced oxidation Fenton-like water treatment technology: a mini review, Env. Funct. Mat. 3 (1) (2024) 59–71.
[15] Q. Liu, H. Li, H. Zhang, Z. Shen, H. Ji, The role of Cs dopants for improved activation of molecular oxygen and degradation of tetracycline over carbon nitride, Chin. Chem. Lett. 33 (2022) 4756–4760.
[16] A.R. Tehrani-Bagha, T. Balchi, Catalytic wet peroxide oxidation, in: Advanced oxidation processes for waste water treatment, Elsevier, 2018, pp. 375–402.
[17] P. García-Muñoz, C. López-Maxías, S. Guerra-Rodríguez, J. Carbajo, J.A. Casas, J. Rodríguez-Chueca, Photocatalytic activation of peroxymonosulfate using ilmenite (FeTiO3) for Enterococcus faecalis inactivation, J. Environ. Chem. Eng. 10 (2022) 108231.
[18] P. Garcia-Muñoz, F. Fresno, C. Lefevre, D. Robert, N. Keller, Influence of the solid titanium source on the activity of La1− xTixFeO3 photo-CWPO catalysts under UV-A light, Catal. Today 413 (2023) 113974.
[19] J. Wang, J. Yao, L. Zhu, C. Gao, J. Liu, S. She, X. Wu, A novel Fe-rectorite composite catalyst synergetic photoinduced peroxymonosulfate activation for efficient degradation of antibiotics, Chemosphere 289 (2022) 133211.
[20] P. García-Muñoz, G. Pliego, J.A. Zazo, A. Bahamonde, J.A. Casas, Ilmenite (FeTiO3) as low cost catalyst for advanced oxidation processes, J. Environ. Chem. Eng. 4 (2016) 542–548.
[21] P.V. Gosavi, R.B. Biniwale, Pure phase LaFeO3 perovskite with improved surface area synthesized using different routes and its characterization, Mater. Chem. Phys. 119 (2010) 324–329.
[22] J. Rodríguez-Chueca, M.I. Polo-López, R. Mosteo, M.P. Ormad, P. Fernandez-Ibanez, Disinfection of real and simulated urban wastewater effluents using a mild solar photo-Fenton, Appl Catal B 150 (2014) 619–629.
[23] E.J.J. Laviron, General expression of the linear potential sweep voltammogram in the case of diffusionless electrochemical systems, J. Electroanal. Chem. Interfacial Electrochem. 101 (1979) 19–28.
[24] J.-F. Ma, Y.-N. Hou, J. Guo, H.M.A. Sharif, C. Huang, J. Zhao, H. Li, Y. Song, C. Lu, Y. Han, Rational design of biogenic PdxAuy nanoparticles with enhanced catalytic performance for electrocatalysis and azo dyes degradation, Environ. Res. 204 (2022) 112086.
[25] S. Ng, K. Ghosh, J. Vyskocil, M. Pumera, Two-dimensional vanadium sulfide flexible graphite/polymer films for near-infrared photoelectrocatalysis and electrochemical energy storage, Chem. Eng. J. 435 (2022) 135131.
[26] B.A. Koiki, B.O. Orimolade, B.N. Zwane, O.V. Nkwachukwu, C. Muzenda, D. Nkosi, O.A. Arotiba, The application of FTO-Cu2O/Ag3PO4 heterojunction in the photoelectrochemical degradation of emerging pharmaceutical pollutant under visible light irradiation, Chemosphere 266 (2021) 129231.
[27] O.V. Nkwachukwu, C. Muzenda, B.O. Ojo, B.N. Zwane, B.A. Koiki, B.O. Orimolade, D. Nkosi, N. Mabuba, O.A. Arotiba, Photoelectrochemical degradation of organic pollutants on a La3+ doped BiFeO3 perovskite, Catalysts 11 (2021) 1069.
[28] L. Zhang, X. Hao, J. Li, Y. Wang, Z. Jin, Unique synergistic effects of ZIF-9 (co)-derived cobalt phosphide and CeVO4 heterojunction for efficient hydrogen evolution, Chin. J. Catal. 41 (2020) 82–94.
[29] M. Lashgari, M. Ghanimati, Pollutant photo-conversion strategy to produce hydrogen green fuel and valuable sulfur element using H2S feed and nanostructured alloy photocatalysts: Ni-dopant effect, energy diagram and photo-electrochemical characterization, Chem. Eng. Res. Des. 162 (2020) 85–93.
[30] P. Garcia-Muñoz, C. Lefevre, D. Robert, N. Keller, Ti-substituted LaFeO3 perovskite as photoassisted CWPO catalyst for water treatment, Appl Catal B 248 (2019) 120–128.
[31] J. Wang, S. Wang, Activation of persulfate (PS) and peroxymonosulfate (PMS) and application for the degradation of emerging contaminants, Chem. Eng. J. 334 (2018) 1502–1517.
[32] X. Ao, W. Liu, W. Sun, M. Cai, Z. Ye, C. Yang, Z. Lu, C. Li, Medium pressure UV-activated peroxymonosulfate for ciprofloxacin degradation: kinetics, mechanism, and genotoxicity, Chem. Eng. J. 345 (2018) 87–97.
[33] B. Neppolian, M.V. Shankar, V. Murugesan, Semiconductor assisted photodegradation of textile dye, 2002.
[34] M. Karaca, C. Karaca, Z. Eroğlu, M. Sevim, S. Karaca, Usage of MnFe2O4-rGO nanocomposite as efficient Fenton catalyst for tetracycline removal by heterogeneous sono Fenton process: characterizations, catalytic performance assessment, and mechanism, Mater. Chem. Phys. 309 (2023) 128379.
[35] H. Salari, H. Yaghmaei, Z-scheme 3D Bi2WO6/MnO2 heterojunction for increased photoinduced charge separation and enhanced photocatalytic activity, Appl. Surf. Sci. 532 (2020) 147413.
[36] D. Haro, P. García-Muñoz, M. Mola, F. Fresno, J. Rodríguez-Chueca, Atacamite (Cu2Cl (OH) 3) as catalyst of different AOPs for water disinfection, Catal. Today 429 (2024) 114496.
[37] J. Cao, L. Lai, B. Lai, G. Yao, X. Chen, L. Song, Degradation of tetracycline by peroxymonosulfate activated with zero-valent iron: performance, intermediates, toxicity and mechanism, Chem. Eng. J. 364 (2019) 45–56.
[38] Y. Zhang, Y.-G. Zhao, Y. Hu, M. Gao, L. Guo, J. Ji, Insight in degradation of tetracycline in mariculture wastewater by ultraviolet/persulfate advanced oxidation process, Environ. Res. 212 (2022) 113324.
[39] C. Tan, Y. Shen, X. Jian, S. Xu, L. Deng, H. He, X. Min, M. Chen, Performance of the solar/peroxymonosulfate process in (waste) water treatment: abatement of micropollutants, roles of reactive oxygen species, and formation of disinfection by-products, Environ Sci (Camb) 9 (2023) 146–160.

[40] X. Ao, W. Liu, W. Sun, M. Cai, Z. Ye, C. Yang, Z. Lu, C. Li, Medium pressure UV-activated peroxymonosulfate for ciprofloxacin degradation: kinetics, mechanism, and genotoxicity, Chem. Eng. J. 345 (2018) 87–97.
[41] P. Neta, R.E. Huie, A.B. Ross, Rate constants for reactions of inorganic radicals in aqueous solution, J. Phys. Chem. Ref. Data Monogr. 17 (1988) 1027–1284.
[42] D. Kiejza, U. Kotowska, W. Polińska, J. Karpińska, Peracids-new oxidants in advanced oxidation processes: the use of peracetic acid, peroxymonosulfate, and persulfate salts in the removal of organic micropollutants of emerging concern– a review, Sci. Total Environ. 790 (2021) 148195.
[43] Q. Wang, Y. Shao, N. Gao, W. Chu, X. Shen, X. Lu, J. Chen, Y. Zhu, Degradation kinetics and mechanism of 2, 4-Di-tert-butylphenol with UV/persulfate, Chem. Eng. J. 304 (2016) 201–208.
[44] L. Huang, T.G.S. Denis, Y. Xuan, Y.-Y. Huang, M. Tanaka, A. Zadlo, T. Sarna, M. R. Hamblin, Paradoxical potentiation of methylene blue-mediated antimicrobial photodynamic inactivation by sodium azide: role of ambient oxygen and azide radicals, Free Radic. Biol. Med. 53 (2012) 2062–2071.
[45] F. Puga, J.A. Navío, M.C. Hidalgo, A critical view about use of scavengers for reactive species in heterogeneous photocatalysis, Appl. Catal. A Gen. 685 (2024) 119879.
[46] D. Xia, H. He, H. Liu, Y. Wang, Q. Zhang, Y. Li, A. Lu, C. He, P.K. Wong, Persulfate-mediated catalytic and photocatalytic bacterial inactivation by magnetic natural ilmenite, Appl Catal B 238 (2018) 70–81.
[47] J. Rodríguez-Chueca, S. Guerra-Rodriguez, J.M. Raez, M.-J. Lopez-Munoz, E. Rodriguez, Assessment of different iron species as activators of S2O82-and HSO5-for inactivation of wild bacteria strains, Appl Catal B 248 (2019) 54–61.
[48] J. Rodríguez-Chueca, S. Giannakis, M. Marjanovic, M. Kohantorabi, M.R. Gholami, D. Grandjean, L.F. de Alencastro, C. Pulgarín, Solar-assisted bacterial disinfection and removal of contaminants of emerging concern by Fe2+−activated HSO5-vs. S2O82-in drinking water, Appl Catal B 248 (2019) 62–72.